FEBS Letters 588 (2014) 4404–4412

journal homepage: www.FEBSLetters.org

Oxytocinergic circuit from paraventricular and supraoptic nuclei to arcuate POMC neurons in hypothalamus

Yuko Maejima [a,b], Kazuya Sakuma [a], Putra Santoso [a], Darambazar Gantulga [a], Kenichi Katsurada [a], Yoichi Ueta [c], Yuichi Hiraoka [d], Katsuhiko Nishimori [d], Shigeyasu Tanaka [e], Kenju Shimomura [a,b], Toshihiko Yada [a,f,*]

[a] Division of Integrative Physiology, Department of Physiology, Jichi Medical University School of Medicine, Shimotsuke, Tochigi 329-0498, Japan
[b] Department of Electrophysiology and Oncology, Fukushima Medical University School of Medicine, Fukushima 960-1295, Japan
[c] Department of Physiology, School of Medicine, University of Occupational and Environmental Health, Kitakyushu 807-8555, Japan
[d] Department of Molecular and Cell Biology, Graduate School of Agricultural Science, Tohoku University, Miyagi 981-8555, Japan
[e] Department of Biology, Faculty of Science, Shizuoka University, Ohya 836, Shizuoka 422-8529, Japan
[f] Department of Developmental Physiology, Division of Adaptation Development, National Institute for Physiological Sciences, Okazaki, Aichi 444-8585, Japan

ARTICLE INFO

Article history:
Received 19 June 2014
Revised 7 October 2014
Accepted 9 October 2014
Available online 18 October 2014

Edited by Jesus Avila

Keywords:
Arcuate nucleus
Feeding
Obesity
Oxytocin
Proopiomelanocortin

ABSTRACT

Intracerebroventricular injection of oxytocin (Oxt), a neuropeptide produced in hypothalamic paraventricular (PVN) and supraoptic nuclei (SON), melanocortin-dependently suppresses feeding. However, the underlying neuronal pathway is unclear. This study aimed to determine whether Oxt regulates propiomelanocortin (POMC) neurons in the arcuate nucleus (ARC) of the hypothalamus. Intra-ARC injection of Oxt decreased food intake. Oxt increased cytosolic Ca^{2+} in POMC neurons isolated from ARC. ARC POMC neurons expressed Oxt receptors and were contacted by Oxt terminals. Retrograde tracer study revealed the projection of PVN and SON Oxt neurons to ARC. These results demonstrate the novel oxytocinergic signaling from PVN/SON to ARC POMC, possibly regulating feeding.

1. Introduction

Food intake is regulated by neurons within the hypothalamus of the brain [1]. The arcuate nucleus (ARC) is a key hypothalamic region involved in food intake regulation [2,3]. There are two known distinct populations of ARC neurons that regulate food intake and energy expenditure, being recognized as the first order neurons [1]. One is the neurons that express neuropeptide Y (NPY)/agouti-related peptide (AgRP) [4], and the other is the neurons that express pro-opiomelanocortin (POMC)/cocaine and amphetamine-regulated transcript (CART) [1,5]. α-MSH, derived from POMC, reduces food intake and stimulates energy expenditure via activation of melanocortin 3 and 4 receptors (MC3/4R) [6]. The ARC POMC neurons project to the neurons in the paraventricular nucleus (PVN), the second order neurons, where MC3/4R are abundantly expressed. Mutations in POMC and MC3/4R genes cause rare monogenic human obesity syndromes associated with hyperphagia [7]. These observations reemphasize the importance of POMC neurons and downstream melanocortin pathway in maintaining the proper body weight and food intake. Therefore, elucidation of regulatory mechanism of ARC POMC neurons is prospectively important both in the physiology of energy balance and for the treatment of obesity. Although several regulators of ARC POMC neuron activity, such as leptin, insulin and 5-HT, have been reported [8], other yet unidentified regulatory factors might also be involved.

Oxytocin (Oxt) is a profoundly recognized neurophysial hormone with important peripheral functions including the uterus contraction during labor and milk ejection [9]. In addition, recent studies have indicated important functions of Oxt in the central nervous system (CNS) such as social [10,11] and maternal behavior [12]. Among the reported effects of Oxt in CNS, the capability of Oxt to regulate food intake and energy metabolism attracts the great interest. Oxt is expressed predominantly in PVN and supraoptic nucleus (SON) of the hypothalamus. Intracereberoventricular (ICV) injection of Oxt suppresses food intake in a melanocortin-dependent manner

* Corresponding author at: Division of Integrative Physiology, Department of Physiology, Jichi Medical University School of Medicine, Shimotsuke, Tochigi 329-0498, Japan.
E-mail address: tyada@jichi.ac.jp (T. Yada).

http://dx.doi.org/10.1016/j.febslet.2014.10.010

[13,14]. Furthermore, we have previously shown that Oxt neurons innervate and directly regulate POMC neurons in the nucleus of the solitary tract (NTS) and that the neural pathway from PVN Oxt to NTS POMC neurons mediates the anorexigenic effect of nesfatin-1 [14]. However, possible link of Oxt neurons to the POMC neurons in ARC remains unclear.

In this study we aimed to explore whether the PVN and/or SON Oxt neurons regulate the ARC POMC neurons. The results show that Oxt is a new regulator of ARC POMC neurons and that the PVN and SON Oxt neurons project to ARC POMC neurons.

2. Materials and methods

2.1. Animals

Adult male Wistar rats, transgenic rats bearing an Oxt-monomeric red fluorescent protein 1(mRFP1) fusion transgene [15] (200–250 g body weight), and knock-in mice expressing the fluorescent venus protein under the control of endogenous regulatory region of Oxt receptor (Oxt-R) (Oxt-R venus mouse: approximately 30 g BW) [16] were housed under 12 h dark/light cycle (lights on at

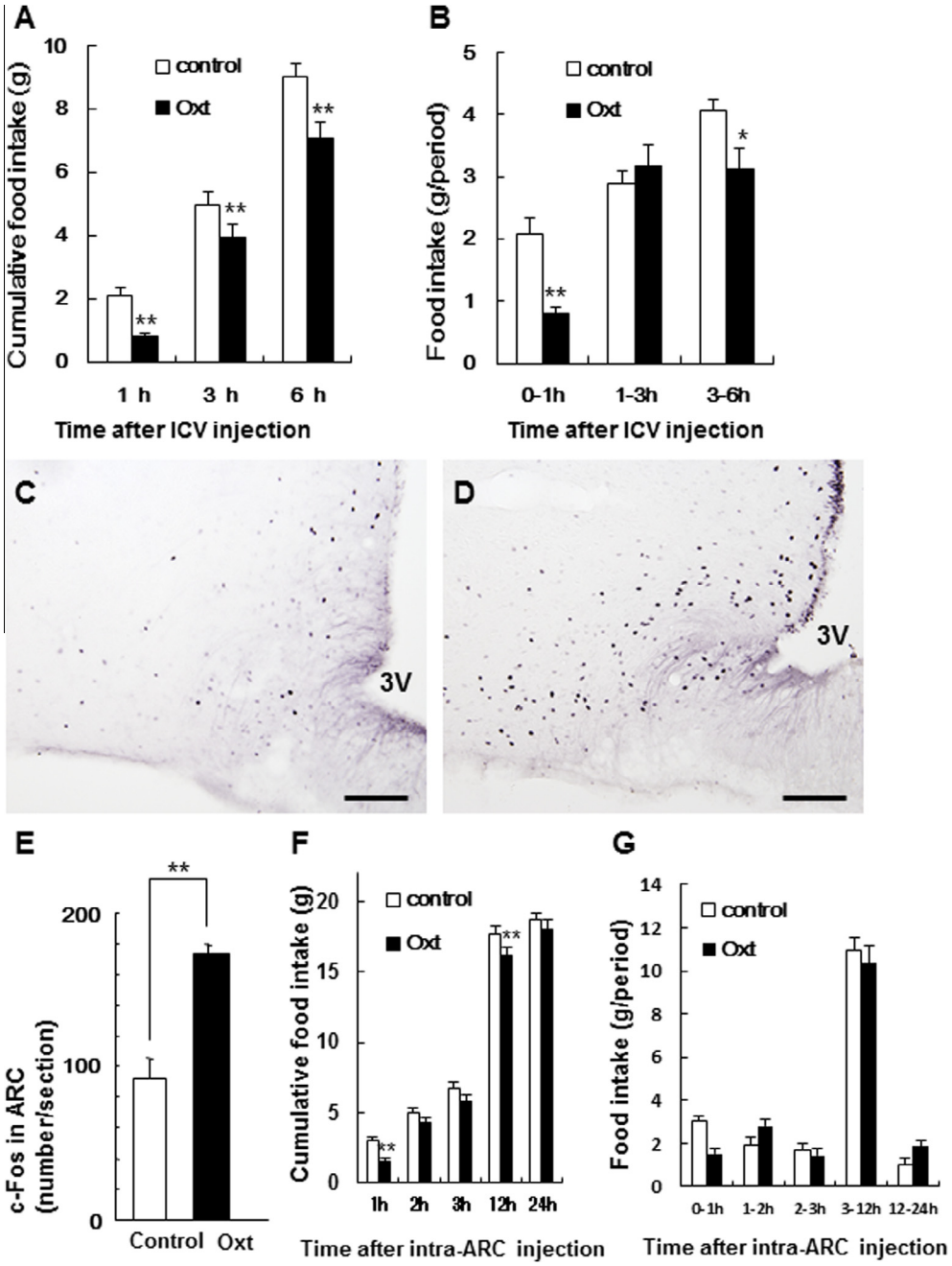

Fig. 1. Lateral ventricle (LV) injection of Oxt suppresses food intake and induces c-Fos expression in ARC, and intra-ARC injection of Oxt suppresses food intake. (A and B) cumulative (A) and periodical (B) food intake after LV injection of vehicle (0.9% NaCl: open bar) or Oxt (filled bar) (4 nmol/5 μl). $n = 10$ for control and 10 for Oxt injected groups. $^{*}P < 0.05$. $^{**}P < 0.01$ vs. control by repeated measures two-way ANOVA by Turkey's post hoc test. (C and D) The representative microphotographs of c-Fos immunostaining in arcuate nucleus (ARC) after LV injection of saline ((C) $n = 3$) or 4 nmol Oxt ((D) $n = 3$). Scale bars indicate 100 μm. (E) Number of c-Fos immunoreactive neurons/section in ARC after injection of 4 nmol Oxt (filled bar) or 5 μl vehicle (open bar). $^{**}P < 0.01$ vs. control by unpaired t-test. (F and G) Cumulative (F) and periodical (G) food intake for 1–24 h after focal injection of vehicle (0.9% NaCl: open bar) or Oxt (0.4 nmol/0.5 μl: filled bar) into ARC ($n = 8$ each). Each bar represents mean ± S.E. $^{**}P < 0.01$ vs. control by repeated measures two-way ANOVA by Turkey's post hoc test.

07:30 and off at 19:30) and temperature controlled (22 °C) conditions and given standard chow (CE-2; Clea, Osaka, Japan) and water *ad libitum*. The animal protocols were approved by the Jichi Medical University Institute of Animal Care and Use Committee.

2.2. ICV and intra-ARC cannulation and measurements of food intake

Rats were anesthetized by intraperitoneal (ip) injection of Avertin (tribromoethanol, 200 mg/kg, ip). For ICV injection, a 26-gauge guide cannula was placed stereotaxically into the lateral ventricle (LV) (0.8 mm caudal to the bregma, 1.5 mm lateral from the midline and 3.2 mm below the surface of the skull). For intra-ARC injection, the cannula was inserted into the ARC (3 mm caudal to the bregma in the midline, 0.3 mm lateral and 9.0 mm below the surface of the skull). The injector needle extended by 0.6 mm beyond the tip of the guide cannula for the LV and intra ARC injection. Rats were allowed to recover from the operation at least for 10 days while they were habituated to handling.

On the day of experiments, food was removed from individual cage 3 h before onset of dark phase. Injection of Oxt into LV (4 nmol/5 μl) or ARC (0.4 nmol/0.5 μl) were performed just before onset of dark phase, and cumulative food intake 1, 3, and 6 h for LV injection and 1, 2, 3, 12 and 24 h for intra ARC injection were measured. To prevent spillage from food container, new chows larger enough compared to slits on container were provided at the beginning of experiment. At the end of the experiments, sections of the hypothalamus were histologically examined to verify the position of the cannulas. LV cannulation was successful in all animals. Intra-ARC cannulation was unsuccessful in four rats and these animals were excluded from the study.

2.3. Staining for c-Fos, POMC, and agouti-related peptide (AgRP)

Animals were deprived of food 3 h before onset of dark cycle until the transcardial perfusion. Animals received injections into the LV with either 4 nmol/5 μl Oxt ($n = 3$) or 5 μl vehicle ($n = 3$) just before the onset of dark cycle. Two hours later, rats were transcardially perfused with 4% paraformaldehyde solution containing 0.2% picric acid. Coronal sections having thickness of 40 μm were cut with the help of a freezing microtome. Sections at 200 μm intervals between −1.7 and −3.3 mm from the bregma were used for immunohistochemistry. For c-Fos staining, anti-c-Fos antiserum (1:5000, sc-52; Santa Cruz, CA) was used following previous report [17].

Double-labeling immunohistochemistry for c-Fos with POMC or AgRP was performed as reported [14]. Rabbit anti-POMC serum (1:5000) [18] or anti-AgRP serum (Phoenix pharmaceuticals Inc. CA, 1:500) was used as the first antibody. The number of c-Fos immunoreactive (IR) cells per section was counted for the ARC between −1.7 and −3.3 mm from bregma. The count in a section was averaged for all sections in ARC in each animal, yielding an individual datum. For double immunostaining, c-Fos-IR cells, POMC- or AgRP-IR cells, and dually IR cells were counted in the sections containing ARC. The fraction of c-Fos-IR cells in

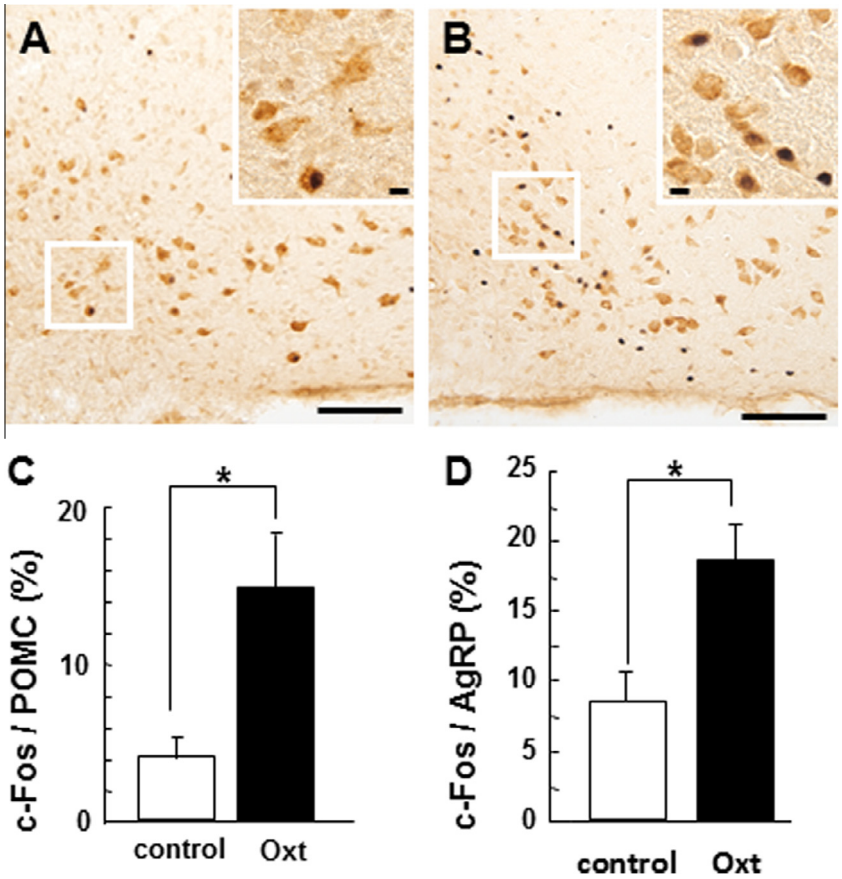

Fig. 2. Oxt induces c-Fos expression in ARC POMC neurons. (A and B) Representative images of double immunostaining of c-Fos and POMC in ARC after LV injection of saline ((A) $n = 3$) or 4 nmol Oxt ((B) $n = 3$). Scale bars indicate 100 μm and those in separated pictures with large magnification 10 μm. (C) Percentage of c-Fos positive neurons in ARC POMC neurons after LV injection of 4 nmol Oxt (filled bar) or 5 μl vehicle (open bar). (D) Percentage of c-Fos positive neurons in ARC AgRP neurons after LV injection of 4 nmol Oxt (filled bar: $n = 3$) or 5 μl vehicle (open bar: $n = 4$). Each bar represents mean ± S.E. $^*P < 0.05$ compared to control by unpaired t-test.

POMC/AgRP-IR cells, expressed as percentage, was averaged for all sections.

2.4. Observation of oxytocin receptors in POMC neurons in ARC

Oxt-R venus mice [16] were perfused with 4% paraformaldehyde (PFA) in 0.1 M phosphate buffer (PB). Coronal 40 μm sections between −1.34 mm to −1.94 mm from bregma were incubated overnight with rabbit anti-POMC serum [18] diluted 1:5000 at 4 °C. Then sections were incubated with Alexa 594 goat anti-rabbit IgG (Molecular Probes, Carlsbad, CA; 1:500). Confocal fluorescence images were acquired with a confocal laser-scanning microscope (Fluoreview FV1000-TO; Olympus, Tokyo Japan).

2.5. Preparation of single neurons from ARC

Single neurons from male Wistar rats aged 6 weeks were prepared from ARC according to previous reports [19,20] with slight modification. Briefly, brain slices were prepared and the entire ARC areas were punched out in Krebs-Ringer bicarbonate buffer solution (KRB). The tissues were incubated with 20 units/ml papain (Sigma Chemical, St. Louis, MO), 1 mM cystein, 0.015 mg/ml deoxyribonuclease and 0.75 mg/ml BSA in KRB containing 1 mM glucose for 15 min at 36 °C in a shaking water bath. Following gentle trituration, the cell suspension was washed with KRB by centrifugation at 750 rpm for 5 min. The cells were re-suspended in KRB and distributed onto non-coating coverglasses. The cells were kept in a humidified chamber at 30 °C until measurements.

2.6. Measurement of $[Ca^{2+}]_i$ and subsequent immunocytochemistry in single neurons

We used the method of physiological analysis of species-specified single cells [21], which is composed of $[Ca^{2+}]_i$ measurements and subsequent immunostaining. $[Ca^{2+}]_i$ was measured by ratiometric fura-2 microfluorometry and imaging as previously reported [20,22]. Briefly, neurons were incubated with 2 μM fura-2/AM (Dojin chemical, Kumamoto, Japan) for 1 h at room temperature. Then, the neurons were mounted in a chamber and superfused with KRB at 1 ml/min at 33 °C. Fluorescence images due to excitation at 340 and 380 nm were detected with ICCD camera, and the ratio images were produced by Argus-50 (Hamamatsu Photonics Co., Hamamatsu, Japan).

For immunocytochemistry after $[Ca^{2+}]_i$ measurements, single neurons were fixed in 4% PFA for overnight, and then incubated overnight with rabbit antiserum against POMC [18] at 1:5000 dilution at 4 °C, following previous reports [20,22]. $[Ca^{2+}]_i$ result of each cell was correlated with its corresponding immunocytochemical result, based on photographs of cells taken at the end of $[Ca^{2+}]_i$ imaging.

2.7. Criteria for $[Ca^{2+}]_i$ responses and their inhibition

When changes in ratio (F340/F380) took place within 5 min after administration of agents and their amplitudes were 0.4 ratio unit or larger, they were considered as responses, as previously reported [14,17,20]. When Oxt-R antagonist, H4928 ($[d(CH_2)^1_5$, $Tyr(Me)^2$, $Orn^8]$-Oxt) (Bachem, Budendorf, Switzerland), suppressed the Oxt-induced $[Ca^{2+}]_i$ increase by 40% or greater, it was considered as suppression. Amplitudes of $[Ca^{2+}]_i$ responses were

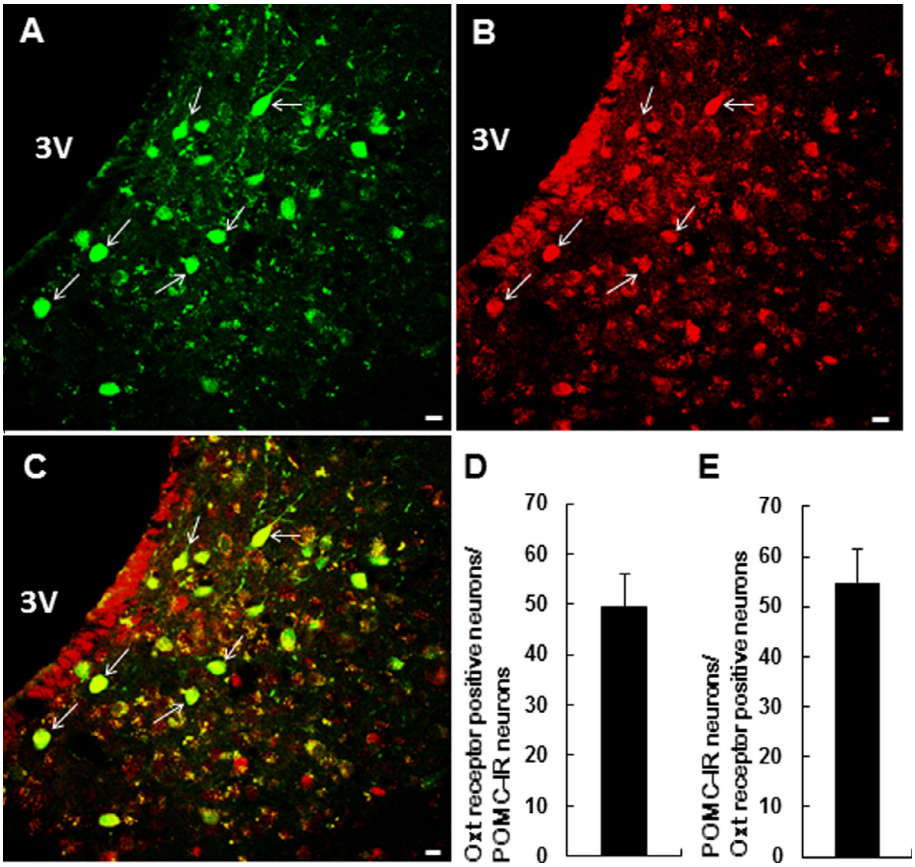

Fig. 3. The expression of Oxt receptor (Oxt-R) in POMC neurons in ARC. (A) Distribution of Oxt-R and (B) POMC neurons in ARC of Oxt-R-venus knock in mice. White arrows indicate neurons double positive for Oxt-R and POMC. (C) Merged image of (A) and (B). Scale bars indicate 10 μm. (D) Percentage of Oxt-R positive neurons in POMC positive neurons. (E) Percentage of POMC neurons in Oxt-R positive neurons.

calculated by subtracting prestimulatory basal $[Ca^{2+}]_i$ ratio from peak $[Ca^{2+}]_i$ ratio.

2.8. Projection of Oxt terminal to ARC POMC neurons

Oxt-mRFP rats were anesthetized by ip injection of Avertin (tribromoethanol, 200 mg/kg) before brains were removed. The brain sections between −1.78 and −3.25 mm from bregma were prepared. Sections were incubated with primary antibody, rabbit anti-POMC antiserum (1:5000) [18] for overnight at 4 °C, followed by incubation for 40 min with secondary antibodies, Alexa 488 goat anti-rabbit IgG (Molecular Probes, Carlsbad, CA; 1:500). Sections were mounted with the medium containing DAPI (VECTASHIELD; Vector, CA). Confocal fluorescence images were acquired with a confocal laser-scanning microscope (Fluoreview FV1000-TO; Olympus, Tokyo, Japan).

2.9. Injection of retrograding tracer

A retrograde tracer, cholera toxin subunit B Alexa Fluor 488 (CTB: Invitrogen, CA), was used to identify the pathway connecting ARC and PVN Oxt neurons in Oxt-mRFP rats. CTB, 0.5 μl of 0.5 mg/ml, was acutely injected into unilateral ARC (3 mm caudal to the bregma, 0.3 mm lateral from midline and 9.4 mm below the surface of the skull) under anaesthesia. Similarly, CTB was injected into median eminence (ME: 3 mm caudal to the bregma in the midline and 9.8 mm below the surface of the scull). Four days after injection of CTB, animals were perfused with 4% PFA containing 0.2% picric acid. Brain sections were made by cutting in freezing microtome. Confocal fluorescence images of Oxt and CTB labels were acquired with a confocal laser-scanning microscope (Fluoreview FV1000-TO; Olympus, Tokyo, Japan). Accuracy of injection was confirmed histologically.

2.10. Statistical analysis

Data are expressed as means ± S.E. Data were analyzed by unpaired or paired Student's *t* test or by repeated measures two-way ANOVA with treatment (saline vs. Oxt) and time as factors. Post hoc multiple comparisons were made using Turkey's post hoc test. $P < 0.05$ was considered significant.

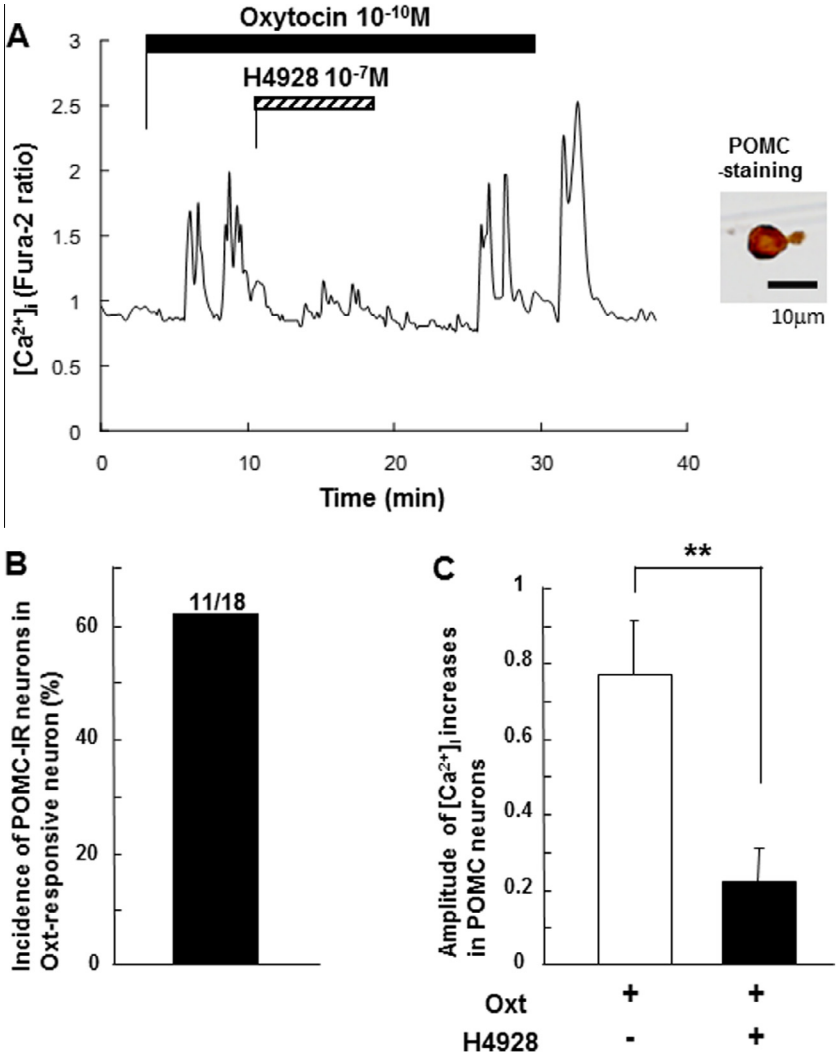

Fig. 4. Oxt induces $[Ca^{2+}]_i$ increases in ARC POMC neurons via Oxt-R. (A) Oxt at 10^{-10} M increased $[Ca^{2+}]_i$, and the $[Ca^{2+}]_i$ increase was suppressed by Oxt-R blocker H4928 at 10^{-7} M (left panel) in a neuron isolated from adult male rat. Superfusates contained 1 mM glucose. This neuron was subsequently shown to be immunoreactive to POMC (right panel). Scale bar = 10 μm. (B) Incidence of $[Ca^{2+}]_i$ responses to Oxt in ARC POMC neurons, as expressed by percentage. (C) The amplitude of $[Ca^{2+}]_i$ response to Oxt in the absence (white bar) and presence of H4928 (black bar). $^{**}P < 0.01$ by paired *t*-test.

3. Results

3.1. Oxt targets ARC POMC neurons

LV Oxt injection significantly reduced cumulative food intake ($F_{1,36} = 63.24$, $P < 0.01$) (Fig. 1A) and periodical food intake ($F_{1,36} = 4.11$, $P < 0.01$) (Fig. 1B). Periodical food intake during 0–1 h, 1–3 h and 3–12 h in Oxt-treated group was 38% ($P < 0.01$), 110% and 77% ($P < 0.05$) of that in control group, respectively. LV Oxt injection significantly induced c-Fos expression in the ARC of hypothalamus (Fig. 1C–E), suggesting that ARC is targeted by Oxt. Furthermore, intra-ARC injection of Oxt significantly reduced cumulative food intake at 1 and 12 h after injection ($F_{1,56} = 18.47$, $P < 0.01$) (Fig. 1F), and periodical food intake during 0–1 h tended to decrease (Fig. 1G). Periodical food intake during 0–1 h, 1–2 h, 2–3 h, 3–12 h and 12–24 h in Oxt-treated group was 50%, 145%, 85%, 95% and 187% of that in control group, respectively (not statistically significant in all time periods). These results indicate that anorexigenic effect of LV Oxt injection is greater than that of intra-ARC Oxt injection, suggesting that ARC activation mediates a part, but not all, of food intake reduction by LV Oxt injection.

The LV injection of Oxt, compared to vehicle injection, significantly increased c-Fos expression in ARC POMC (Fig. 2A and B) and AgRP neurons. The expression of c-Fos was observed in 14.7% of POMC neurons in Oxt injected group, compared to 4.1% in control group (Fig. 2C). C-Fos expression was also observed 18.5% and 8.0% of AgRP neurons in Oxt injected and control groups, respectively (Fig. 2D). These data indicate that POMC neuron is one of the neurons influenced by Oxt in ARC.

3.2. ARC POMC neurons express Oxt-R and are directly activated by Oxt

To study the localization of Oxt receptors in ARC POMC neurons, we used Oxt-R venus mice [16] combined with immunohistochemistry for POMC. Oxt-R were widely distributed in ARC (Fig. 3A). Confocal images confirmed that a large number of POMC-immunoreactive (IR) neurons express Oxt-R (Fig. 3A–C). Fifty percent of POMC-IR neurons expressed Oxt-R (Fig. 3D), and 55% of Oxt-R-expressing neurons were POMC-IR neurons (Fig. 3E).

Administration of 10^{-10} M Oxt increased $[Ca^{2+}]_i$ in a single ARC neuron (Fig. 4A, left) that was subsequently shown to be IR to POMC (Fig. 4A, right). A large fraction of the neurons (11/18) that responded to Oxt were POMC-IR neurons (Fig. 4B). The $[Ca^{2+}]_i$ increase in response to Oxt was significantly suppressed by administration of OxtR-antagonist, H4928 (Fig. 4A and C).

3.3. PVN and SON Oxt neurons project to ARC POMC neurons

Confocal images of immunostaining of POMC neurons (Fig. 5A) in Oxt-mRFP rats indicated that the Oxt terminals (Fig. 5B) were in contact with the POMC neurons in ARC (Fig. 5A–D).

It was confirmed that the retrograde tracer CTB was injected specifically into ARC region without significant diffusion to other regions including the ventromedial hypothalamic nucleus (VMH) (Fig. 6C). The CTB fluorescence was detected specifically and intensely in ipsilateral PVN and SON on the same side of injection (Fig. 6D). Few fluorescence was detected in the contralateral side of PVN and SON (Fig. 6D). In contrast, when CTB was injected into median eminence (Fig. 6E) with diffusion into 3V (Fig. 6F), no CTB signals were detected in PVN (Fig. 6G) and SON. The result suggests that if ARC-injected CTB diffused into 3V, it would have no effect on the CTB signals in PVN and SON, reinforcing that CTB signals in PVN and SON originate from ARC. When analyzed at the neuron level, CTB fluorescence was detected in both parvocellular and magnocellular neurons in the PVN (Fig. 6H) and throughout the SON (Fig. 6N). In PVN, 29% of CTB fluorescence-positive neurons were identified as Oxt neurons (Fig. 6H–M and Q), and conversely 27% of Oxt neurons were CTB fluorescence-positive (Fig. 6H–M and R). In the SON, 24% of CTB fluorescence-positive neurons were Oxt neurons (Fig. 6N–Q), and 21% of Oxt neurons were CTB

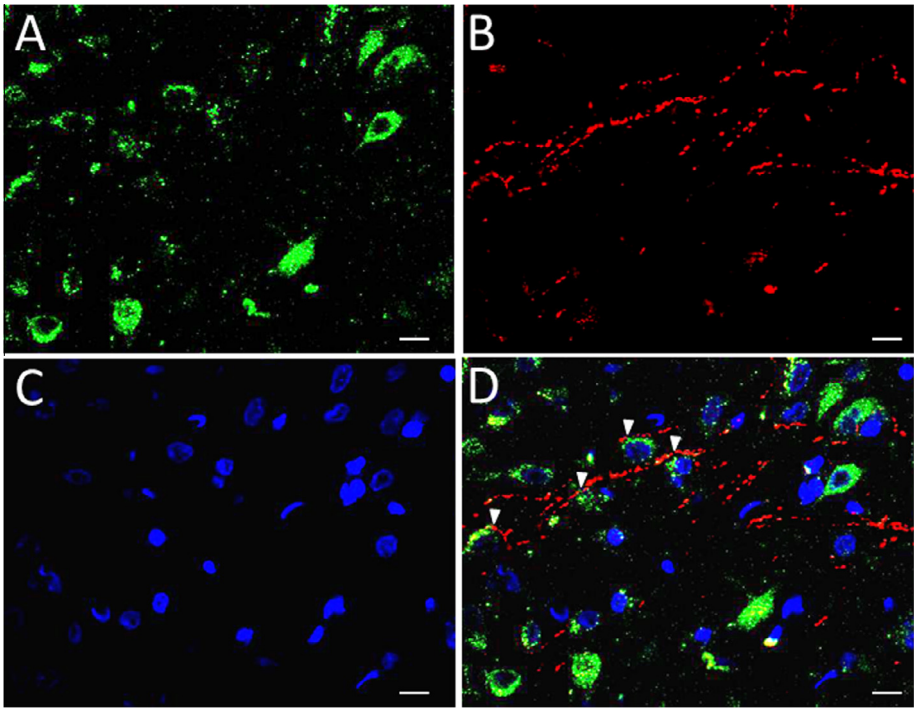

Fig. 5. The terminal of Oxt contact to ARC POMC neurons. (A) Confocal images of POMC-IR neurons, (B) Oxt terminals, and (C) DAPI nuclear counter staining, and (D) merged images of (A)–(C) in ARC of Oxt-mRFP rats. White arrow heads indicate the contact of Oxt terminals to POMC neurons. Scale bars indicate 10 μm.

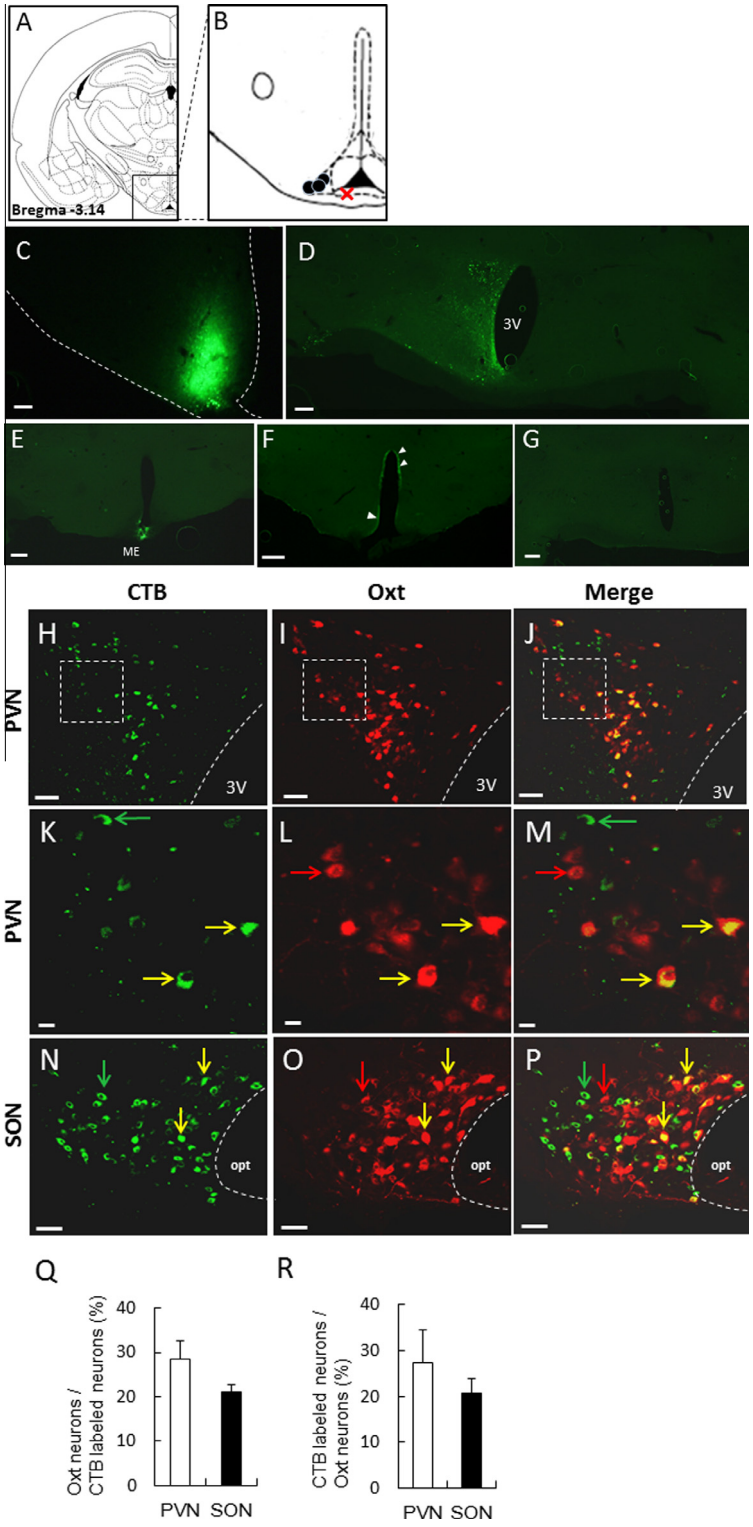

Fig. 6. Oxt neurons in PVN and SON project to the ARC. (A and B) The brain map of the coronal level including injection sites (A), and larger scale map showing choleratoxin subunit B (CTB) injection position in ARC (B). Black circles show each injection positions in ARC and red cross shows the position of injection into median eminence (ME) for negative control. (C) Representative injection site of CTB in ARC. (D) Tracer positive regions in the hypothalamus at 4 days after CTB injection into ARC. Scale bars in (C) and (D) indicate 100 μm. (E–G) CTB injection site in ME for negative control (E). When CTB was injected to ME with diffusion to 3V, CTB signals were present in ependymal cells (white arrows) (F) but absent in PVN (G). (H and J) CTB positive neurons (H), Oxt neurons (I), and their merge (J) in PVN. Scale bars indicate 50 μm. (K–M) Areas designated by white squares in (H)–(J) are shown with expanded scale. Green and red allows indicate CTB and Oxt single-positive neurons, respectively. Yellow arrows indicate CTB and Oxt double-positive neurons. Scale bars indicate 10 μm. (N–P) CTB positive neurons (N), Oxt neurons (O), and their merge (P) in SON. Green and red allows indicate CTB and Oxt single-positive neurons, respectively. Yellow arrows indicate CTB and Oxt double-positive neurons. Scale bars indicate 50 μm. 3V: 3rd ventricle, opt: optic tract. (Q) The percentage of Oxt neurons among CTB labeled neurons in PVN (open bar) and SON (filled bar). (R) The percentage of CTB labeled neurons among Oxt neurons in PVN (open bar) and SON (filled bar).

fluorescence-positive (Fig. 6N–P and R). The result identifies the PVN and SON Oxt neurons as the sources of Oxt projection in ARC.

4. Discussion

The present study demonstrated a novel oxytocinergic neural pathway from the PVN and SON to the ARC POMC neurons, which could be linked to regulation of feeding.

The important role of Oxt in regulating food intake is well recognized. Recent studies have clarified the specific nuclei that are involved in Oxt-mediated food intake regulation, which include ventral tegmental area (VTA), PVN, ARC, VMH, amygdala and NTS [23–25]. Therefore, ARC appears to be one of several nuclei involved in food intake regulation by Oxt. ICV injection of Oxt may activate neurons expressing Oxt-R in all the reported nuclei whereas intra-ARC injection activate only those in ARC. This could explain our result that ICV injection of Oxt reduced food intake to a larger extent than intra-ARC injection.

It is evident that ARC neurons are one of the key factors for the Oxt-mediated food intake regulation [25]. In the present study, we have identified a chemical coding of neurons in ARC activated by Oxt and projection of Oxt neurons to ARC from PVN and SON.

Immunostaining of POMC neurons in Oxt-R venus mice demonstrated that POMC neurons in ARC express Oxt-R. Moreover, the $[Ca^{2+}]_i$ measurement in single neurons combined with subsequent immunocytochemistry demonstrated that Oxt directly interacts with and increases $[Ca^{2+}]_i$ in ARC POMC neurons and that the $[Ca^{2+}]_i$ increases are suppressed by Oxt-R antagonist, H4928. These results indicate that Oxt directly activates ARC POMC neurons via Oxt-R. In this study, 60% of single PVN neurons that responded to Oxt were identified as POMC neurons, and this incidence is close to that of POMC neurons among Oxt-R positive neurons in ARC (55%). These Ca^{2+} imaging and histological data support the concept that the POMC neuron is a major target of Oxt in ARC.

In this study, the immunostaining of POMC neurons in the ARC of Oxt-mRFP rats confirmed that Oxt neuron terminals contact the POMC neurons in ARC. This is consistent with previous report by electron microscopic observation that the Oxt nerve fibers innervate the neurons IR to β-endorphin, the POMC-derived peptide, in ARC [26].

Recently, it was reported that POMC neurons in the ARC and those in the NTS play different roles in regulating food intake [27]; ARC POMC neurons long-termly while NTS POMC short-termly regulate feeding. However, our present and previous studies [14] taken together indicate that PVN Oxt neurons regulate POMC neurons in both NTS and ARC.

The histological study using retrograde tracer CTB [28] have shown that Oxt neurons in PVN and SON project to ARC. The intensive histological studies in 1980s established that a population of PVN Oxt neurons termed magnocellular neurons send axon terminals to the pituitary gland, being recognized as the neuroendocrine function, and the other population termed parvocellular neurons project to various brain regions [29], while SON neurons send axon terminals to the pituitary gland. Our finding that PVN Oxt neurons project to ARC fits with the classic concept of the parvocellular neuron in PVN. In considering pivotal roles of both Oxt and POMC in feeding, the projection of PVN Oxt to ARC POMC might participate in regulation of feeding. In contrast, our data showing that a part of SON Oxt neurons also project to ARC suggest a possibility that a subpopulation of SON neurons operate a novel function of neurotransmission to ARC and possibly other brain areas. However, the physiological significance of the Oxt neuronal projections from PVN and SON to ARC POMC neurons, shown in this study, still remains unclear, and further study is required to clarify it.

In this study, non-POMC neurons in ARC also expressed Oxt-R, and Oxt altered $[Ca^{2+}]_i$ in non-POMC neurons. The neurochemical identity of the ARC non-POMC neurons that express Oxt-R and respond to Oxt remains unclear. Similarly to our study, Krashes et al. has recently shown that pituitary adenylate cyclase-activating polypeptide (PACAP) and thyrotropin-releasing peptide (TRH) positive neurons in PVN project to orexigenic NPY/AgRP neurons in ARC and are activated by hunger [30]. Our result of c-Fos expression in AgRP neurons also supports these report. These findings by us and by Krashes et al. [30] suggest an involvement of the PVN to ARC neural pathways in regulation of hypothalamic functions including feeding.

The present study demonstrates the novel oxytocinergic pathway from PVN/SON to ARC POMC possibly regulating food intake, which suggests the neural signaling in the reverse direction, from the second order PVN Oxt neuron to the first order ARC POMC neuron.

Disclosure statement

The authors have nothing to disclose.

Acknowledgments

Authors wold like to thank Dr. Ken Fujiwara in Jichi Medical University for histological advice, and Dr. Juris Galvanovskis (Oxford Univ, UK) for the critical reading and comments. This work was supported by Grant-in-Aid for Scientific Research (C) (24591341) from Japan Society for the Promotion of Science (JSPS), Memorial Foundation for Female Natural Scientists and Kowa Life Science Foundation, Japan to Y.M. This study was supported by Grant-in-Aid for Scientific Research (B) (23390044) and Challenging Exploratory Research (22659044, 26670453) from JSPS, Strategic Research Program for Brain Sciences (10036069) by the Ministry of Education, Culture, Sports, Science and Technology of Japan (MEXT), MEXT-Supported Program for the Strategic Research Foundation at Private Universities 2011–2015 and 2013–2017, and a grant from Salt Science Research Foundation, No. 1434 to T.Y. This study was subsidized by JKA through its promotion funds from KEIRIN RACE to T.Y.

References

[1] Schwartz, M.W., Woods, S.C., Porte Jr., D., Seeley, R.J. and Baskin, D.G. (2000) Central nervous system control of food intake. Nature 404 (6778), 661–671.
[2] Elmquist, J.K., Coppari, R., Balthasar, N., Ichinose, M. and Lowell, B.B. (2005) Identifying hypothalamic pathway controlling food intake, body weight, and glucose homeostasis. J. Comp. Neurol. 4921 (1), 63–71.
[3] Parker, J.A. and Bloom, S.R. (2012) Hypothalamic neuropeptides and the regulation of appetite. Neuropharmacology 63 (1), 18–30.
[4] Henry, B.A., Rao, A., Ikenasio, B.A., Mountjoy, K.G., Tilbrook, A.J. and Clarke, I.J. (2001) Differential expression of cocaine- and amphetamine-regulated transcript and agouti related-protein in chronically food-restricted sheep. Brain Res. 918 (1–2), 40–50.
[5] Adam, C.L., Archer, Z.A., Findlay, P.A., Thomas, L. and Marie, M. (2002) Hypothalamic gene expression in sheep for cocain and amphetamine-regulated transcript, pro-opiomelanocortin, neuropeptide Y, agouti-related peptide and leptin receptor and responses to negative energy balance. Neuroendocrinology 75 (4), 250–256.
[6] Cone, R.D. (2005) Anatomy and regulation of the central melanocortin system. Nat. Neurosci. 8 (5), 571–578.
[7] Ferooqi, I.S. and O'Rahilly, S. (2004) Monogenic human obesity syndromes. Recent Prog. Horm. Res. 59, 409–424.
[8] Xu, Y., Elmquist, J.K. and Fukuda, M. (2011) Central nervous control of energy and glucose balance: focus on the central melanocortin system. Ann. NY. Acad. Sci. 124, 1–14.
[9] Kiss, A. and Mikkelsen, J.D. (2005) Oxytocin-anatomy and functional assignments: a minireview. Endocr. Regul. 39 (3), 97–105.
[10] Kosfeld, M., Heinrichs, M., Zak, P.J., Fischbacher, U. and Fehr, E. (2005) Oxytocin increases trust in humans. Nature 435 (7042). 673-65.
[11] Miller, G. (2013) Neuroscience. The promise and perils of oxytocin. Science 339 (6117), 267–269.
[12] Jin, D., Liu, H.X., Hirai, H., Torashima, T., Nagai, T., Lopatina, O., Shnayder, N.A., Yamada, K., Noda, M., Seike, T., Fujita, K., Takasawa, S., Yokoyama, S., Koizumi,

K., Shiraishi, Y., Tanaka, S., Hashii, M., Yoshihara, T., Higashida, K., Islam, M.S., Yamada, N., Hayashi, K., Noguchi, N., Kato, I., Okamoto, H., Matsushima, A., Salmina, A., Munesue, T., Shimizu, N., Mochida, S., Asano, M. and Higashida, H. (2014) CD38 is critical for social behaviour by regulating oxytocin secretion. Nature 446 (7131), 41–45.

[13] Arletti, R., Benelli, A. and Bertolini, A. (1989) Influence of oxytocin on feeding behaviour in the rat. Peptides 10 (1), 89–93.

[14] Maejima, Y., Sedbazar, U., Suyama, S., Kohno, D., Onaka, T., Takano, E., Yoshida, N., Koike, M., Uchiyama, Y., Fujiwara, K., Yashiro, T., Horvath, T.H., Dietrich, M.O., Tanaka, S., Dezaki, K., Oh-I, S., Hashimoto, K., Shimizu, H., Nakata, M., Mori, M. and Yada, T. (2009) Nesfatin-1-regulated oxytocinergic signalling in the paraventricular nucleus causes anorexia through a leptin-independent melanocortin pathway. Cell Metab. 10 (5), 355–365.

[15] Katoh, A., Fijihara, H., Ohbuchi, T., Onaka, T., Hashimoro, T., Kawata, M., Suzuki, H. and Ueta, Y. (2011) Highly visible expression of an oxytocin-monometric red fluorescent 1 fusion gene in the hypothalamus and posterior pituitary of transgenic rats. Neuroendocrinology 152 (7), 2268–2774.

[16] Yoshida, M., Takayanagi, Y., Inoue, K., Kimura, T., Young, L.J., Onaka, T. and Nishimori, K. (2009) Evidence that oxytocin exerts anxiolytic effects via oxytocin receptor expressed in serotonergic neurons in mice. J. Neurosci. 18 (7), 2259–2271.

[17] Maejima, Y., Iwasaki, Y., Yamaharam, Y., Kodaira, M., Sedbazar, U. and Yada, T. (2011) Peripheral oxytocin treatment ameliorates obesity by reducing food intake and visceral fat mass. Aging (Albany NY) 3 (12), 1168–1177.

[18] Tanaka, S. and Kurosumi, K.A. (1992) Certain step of proteolytic processing of proopiomelanocortin occurs during the transition between two distinct stages of secretory granule maturation in rat anterior pituitary corticotrophs. Endocrinology 131 (2), 779–786.

[19] Muroya, S., Yada, T., Shioda, S. and Takigawa, M. (1999) Glucose-sensitive neurons in the rat arcuate nucleus contain neuropeptide Y. Neurosci. Lett. 264 (1–3), 113–116.

[20] Kohno, D., Nakata, M., Maekawa, F., Fujiwara, K., Maejima, Y., Kuramochi, M., Shimazaki, T., Okano, H., Onaka, T. and Yada, T. (2007) Leptin suppresses ghrelin-induced activation of neuropeptide Y neurons in the arcuate nucleus via phosphatidylinositol 3-kinase- and phosphodiesterase 3-mediated pathway. Endocrinology 148 (5), 2251–2263.

[21] Yada, T., Vigh, S. and Arimura, A. (1993) Pituitary adenylate cyclase activating polypeptide (PACAP) increases cytosolic free Ca^{2+} concentration in folliculo-stellate cells and somatotropes of rat pituitary. Peptides 14 (2), 235–239.

[22] Yada, T., Sakurada, M., Ihida, K., Nakata, M., Murata, F., Arimura, A. and Kikuchi, M. (1994) Pituitary adenylate cyclase activating polypeptide is an extraordinarily potent intra-pancreatic regulator of insulin secretion from islet β-cells. J. Biol. Chem. 269 (2), 1290–1293.

[23] Mullis, K., Kay, K. and Williams, D.L. (2013) Oxytocin action in the ventral tegmental area affects sucrose intake. Brain Res. 1513, 85–91.

[24] Noble, E.E., Billington, C.J., Kotz, C.M. and Wang, C. (2014) Oxytocin in the ventromedial hypothalamic nucleus reduces feeding and acutely increases energy expenditure. Am. J. Physiol. Regul. Integr. Comp. Physiol. 307 (6), 737–745.

[25] Olszewski, P.K., Klockars, A., Olszewska, A.M., Fredriksson, R., Schiöth, H.B. and Levine, A.S. (2010) Molecular, immunohistochemical, and pharmacological evidence of oxytocin's role as inhibitor of carbohydrate but not fat intake. Endocrinology 151 (10), 4736–4744.

[26] Csifáry, A., Ruttner, Z., Tóth, Z. and Palkovits, M. (1992) Oxytocin nerve fibers innervate beta-endorphin neurons in the arcuate nucleus of the rat hypothalamus. Neuroendocrinology 56 (3), 429–435.

[27] Zhan, C., Zhou, J., Feng, Q., Zhang, J.E., Lin, S., Bao, J., Wu, P. and Luo, M. (2013) Acute and long-term suppression of feeding behavior by POMC neurons in the brainstem and hypothalamus, respectively. J. Neurosci. 33 (8), 3624–3632.

[28] Chinnapen, D.J., Hsieh, W.T., te Welscher, Y.M., Saslowsky, D.E., Kaoutzani, L., Brandsma, E., D'Auria, L., Park, H., Wagner, J.S., Drake, K.R., Kang, M., Benjamin, T., Ullman, M.D., Costello, C.E., Kenworthy, A.K., Baumgart, T., Massol, R.H. and Lencer, W.I. (2012) Lipid sorting by ceramide structure from plasma membrane to ER for the cholera toxin receptor ganglioside GM1. Dev. Cell 23 (3), 573–586.

[29] Swanson, L.W. and Sawchenko, P.E. (1980) Paraventricular nucleus: a site for the integration of neuroendocrine and autonomic mechanisms. Neuroendocrinology 31 (6), 410–417.

[30] Krashes, M.J., Shah, B.P., Madara, J.C., Olson, D.P., Strochlic, D.E., Garfield, A.S., Vong, L., Pei, H., Watabe-Uchida, M., Uchida, N., Liberles, S.D. and Lowell, B.B. (2014) An excitatory paraventricular nucleus to AgRP neuron circuit that drives hunger. Nature 507 (7491), 238–249.